IEEE Access
Multidisciplinary | Rapid Review | Open Access Journal

Received May 31, 2018, accepted June 29, 2018, date of publication July 9, 2018, date of current version August 15, 2018.

Digital Object Identifier 10.1109/ACCESS.2018.2854581

Application of the Fast Marching Method for Path Planning of Long-haul Optical Fiber Cables With Shielding

ZENGFU WANG[1], QING WANG[2], BILL MORAN[3], (Member, IEEE), AND MOSHE ZUKERMAN[2], (Fellow, IEEE)

[1]School of Automation, Northwestern Polytechnical University, Xi'an 710072, China
[2]Department of Electronic Engineering, City University of Hong Kong, Hong Kong
[3]Department of Electrical and Electronic Engineering, The University of Melbourne, Melbourne, VIC 3010, Australia

Corresponding author: Moshe Zukerman (m.zu@cityu.edu.hk)

The work described in this paper was primarily supported by a grant from the Research Grants Council of the Hong Kong Special Administrative Region, China [Project No. CityU8/CRF/13G]. It was also supported by a grant from the National Natural Science Foundation of China (NSFC) [Project No. 61503305], by the Natural Science Basic Research Plan in Shaanxi Province of China [Project No. 2018JM6025] and by the Fundamental Research Funds for the Central Universities [Project No. 3102017zy025]. A significant part of the contribution of Z. Wang to this paper was done during his service at City University of Hong Kong.

ABSTRACT This paper provides a method for optimal shielding design and path planning of a long-haul optical fiber cable between two locations on the Earth's surface. The method allows minimization of the cable laying cost including material and labor and the risks of future cable break associated with laying the cable through various areas, including earthquake-prone or other risky areas. Both costs per unit length and risk of cable damage may be different at different locations. Expensive shielding may be important in certain high-risk areas and unnecessary in lower risk areas. We use ground motion intensity to estimate future cable repair rate (our measure of earthquake-related cable damage risk), and a triangulated manifold to represent the surface of the Earth. With laying cost and expected total number of repairs of the cable as the two objectives, we formulate the problem as a multiobjective variational optimization problem. This formulation incorporating multiple design levels for cable shielding is converted into a single objective variational optimization problem by assigning different weights to each objective. The solution path of the later problem is obtained by using the Fast Marching Method (FMM) with an additional minimization step. A new proof of the optimality of FMM for the problem is provided. Numerical results demonstrate that the FMM-based method outperforms existing raster-based algorithms. With billions of US dollars spent yearly on new cables, the potential savings are substantial. Furthermore, the computational complexity of the FMM-based method is $O(N \log(N))$, making it applicable to cables of realistic length.

INDEX TERMS Cost effectiveness, optical fiber cables, path optimization, seismic resilience, multiobjective optimization.

I. INTRODUCTION

Playing an essential role in transmitting information to supply burgeoning demand in the increasingly interconnected world, optical fiber long-haul telecommunication cables are crucial to modern society. The Submarine Cable Map provided by TeleGeography in 2016, shows 293 in-service submarine telecommunication cables or cable systems with total length of around 550,000 miles carry 99% international telecommunications [1], [2].

On the one hand, investments in long-haul optical fiber cables have a significant impact on the economy. On the other hand, breakage or faults of such cables caused by various hazards can lead to severe social and economic consequences. For example, as a result of the 2006 Hengchun (Taiwan) earthquake, 18 cuts were found on eight submarine telecommunication cables: Asia Pacific Cable Network (APCN), Asia Pacific Cable Network 2 (APCN-2), City to City (C2C), China-US Cable Network (CUCN), East Asia Crossing (EAC), FLAG Europe Asia (FEA), FLAG North Asian Loop or Reach North Asian Loop (FNAL/RNAL) and South-East Asia–Middle East–Western Europe 3 (SEA-ME-WE 3 or SMW3), affecting Internet service of several Asian

countries or regions for several weeks [3]. For an indication of financial losses associated with Internet shutdown, we refer to the study that was done in Switzerland in 2005 [4], which concluded that for a modern country such as Switzerland, a loss of 1.2% of annual GDP will incur per one week of Internet shutdown. Moreover, the cost of a repair of a submarine cable ranges between one and three million US dollars [5].

Interestingly, the same eight submarine cables damaged in the 2006 earthquake, were damaged again by the Ryukyu Islands earthquake in 2009. However, following lessons learned from the 2006 earthquake, two new submarine cable systems had been laid further away from Taiwan earthquake prone areas in 2008 and 2009, namely, Trans-Pacific Express (TPE) and TGN-Intra Asia (TGN-IA). These two new cables were not disrupted by the Ryukyu Islands earthquake, and were able to pick up much of the traffic that could not be carried by the damaged cables. As a result, the 2009 Ryukyu Islands earthquake had a far weaker effect on Internet service than the 2006 Hengchun earthquake [3]. While this serves as an example, of how we learn from one disaster how to avoid a future one, it is clearly preferable to incorporate disaster mitigation into the cable route planning and design phase with the aim of avoiding such problems *ab initio*.

Evidently, in addition to construction cost, survivability of cables is an important objective to be considered in cable path planning. There are two ways to improve the survivability of a cable: firstly, to keep the cable a safe distance away from high risk regions resulting in longer cables, and secondly to strengthen the cables with special shielding, or armored components when the cable passes through high risk areas [6], resulting in higher per unit length cable costs.

Different means to strengthen cables are associated with different design levels. In particular, five types of submarine cables [7], light cable, light weight cable, single armored cable, double armored cable and rock armored cable, are commonly used. Light cable has the least protection level and the rock armored cable has the highest protection level. Generally speaking, a higher design level of a cable implies a higher construction cost as it requires more expensive material. Taking account of the two objectives of reducing construction cost and breakage risk, it is important for cable path planners and other stakeholders to determine a suitable (and indeed optimal) trade-off of the cable route that avoids high risk regions and cable design level in the various regions of its path, while minimizing laying cost.

In [8], we considered the optimization of both the path planning and the choice of the cable design levels and formulated the problem as one in multiobjective optimization, where the two conflicting objectives are the construction cost and the risk, measured by the expected number of cable failures. The need for consideration of multiple objectives arises from the fact that there is no clear ''exchange rate'' between the costs associated with cable laying and those associated with cable risk. Different stakeholders may have different exchange rates. For example, a government will assign higher value to the consideration of cable risk than the cable owner because it is more concerned with internet shutdown that may have severe social and economic consequences. A raster-based algorithm, a variant of the label setting algorithm was proposed to solve the multiobjective optimization problem. The interval-partition-based label setting algorithm, which is an approximate algorithm, was presented to provide feasible computational cost for graphs with a large number of nodes. More efficient and, more important, more accurate algorithms are required, especially for path planning and design of cable over long distances, to improve the accuracy and quality of the solution, leading to cost savings and safer design. As in [8], also in this paper, we use the terms *laying* and *construction* interchangeably to mean either laying or construction of cables.

As we mentioned in [9], since different stakeholders have different priorities considering the trade-offs between cable failure risks and initial laying cost, a methodology based on multiobjective optimization can give them a range of optimal solutions on this trade-offs. In this paper, we formulate the optimization of both path planning and choice of the design levels for cables as a multiobjective optimization problem on a two-dimensional triangulated manifold in $\mathbb{R}^3$. Based on the Fast Marching Method (FMM) [10], [11], we provide an optimal and computationally effective approach to solve the multiobjective optimization problem. FMM is useful in overcoming the challenge of path planning of a *continuous* cable while the data is available in *discrete* points. It is also worth mentioning that if we only consider the special case of only one design level of cable in this optimization problem, that is, assuming a homogeneous cable along the route, this problem reduces to the multiobjective variational optimization problem, which we have already solved in [9].

As in [8], our method in this paper can be applied to all the many hazardous scenarios associated with natural causes or human activities that may lead to cable failures as described in [8]. Without loss of generality, for ease of exposition, we assume here that earthquakes are the main cause of cable failures, and we adopt the number of potential repairs along a cable as the measure of risk. This measure, widely accepted in practice as well as in the civil engineering literature, has two key advantages: firstly, it has a strong relationship with repair or reconstruction cost and is associated with societal cost incurred by cable failures and, secondly, it can be quantified in terms of cable repair rate and formulae for cable repair rate based on available ground motion intensity data [12]–[14].

In our context, the designed cable between two given nodes is built on the continuous surface of the Earth, approximately represented by a two-dimensional triangulated manifold in $\mathbb{R}^3$. The fidelity of this model can be improved by finer subdivision, though with consequential increase in computational load. For a region of interest, the ground motion intensity data are acquired by downloading from The United States Geological Survey (USGS, (`https://www.usgs.gov/`)). Next, we show that the formulated multiobjective variational problem incorporating multiple design levels can

be converted into a single objective variational optimization problem by assigning different weights to each objective. We then prove that the solution path of the single objective variational optimization problem can be achieved by realizing the problem as a newly derived extended Eikonal equation and applying the well-known FMM with an additional minimization step. Finally, we generate the approximate Pareto front based on all obtained Pareto optimal solutions, and numerically demonstrate the superiority of the FMM-based method over the method based on interval-partition label setting algorithm of [8] in terms of running times as well as in terms of solution quality. Accordingly, the main novelty and contributions of this paper are as follows.

- The application of FMM cable path planning that takes account of multiple design levels for cable shielding, requiring a new proof that FMM provides an optimal solution for the path of the single objective variational optimization problem. The new proof makes FMM with an additional minimization step applicable to the cable path planning problem, and provides a method that is optimal given the data for cable laying, shielding design and path planning of a long-haul optical fiber cable.
- A numerical demonstration of the superiority of the FMM-based method over the method of [8]. In the two given examples, the improvement achieved by FMM is 3.5-6.6%. Given the billions spent on laying cables around the world, the FMM-based approach has potential for substantial savings. In addition, the computational complexity of FMM-based method is $O(N \log(N))$, making it applicable to cables of realistic length, for which the methods of [8] may not be applicable.

The remainder of the paper is organized as follows. The state-of-the-art and related work are discussed in Section II. The models of laying cost and cable repair are introduced in Section III. In Section IV, we formulate the problem of minimising laying cost and expected total number of repairs for cable design considering path planning and multiple design levels, and we propose our algorithm leveraging on FMM. We apply our proposed algorithm to real-world 3D data, present the corresponding simulation results and compare it numerically to the discrete algorithms [8] in Section V. Finally, conclusions are drawn in Section VI.

II. STATE-OF-THE-ART AND RELATED WORK

Most current approaches to path planning or route selection for cables assume only one design level; that is, cables are homogenous. Two types of approaches, a traditional manual approach based on expert experience [6], [15] and a Geographic Information System (GIS) based path selection approach, are commonly used in the path planning procedures of cables in practice. In fact, the second approach is currently only known to be used for path planning of pipelines [16], but it is potentially applicable also to optical fiber cables.

In the traditional manual approach, planners use data available on the relevant region, for example: detailed maps, charts, aerial photographs, and/or satellite gravity bathymetric data, and produce alternative paths on a large-scale topographical map that connects a starting point and an end point. Then, for a given path, a preliminary survey is conducted along its route to verify its availability and its rationality. If practical obstacles cannot be removed, then the planners consider and explore alternative routes. Finally, the cable path planning is determined by carefully checking all relevant details along the path and comparing between the various alternatives. Such a manual approach depends on subjective analysis based on expert judgment, and since a human cannot check all possible alternatives in realistic time, it cannot guarantee to provide an optimal path. A fast path planning algorithm can help automate at least part of the manual approach.

GIS based path selection approaches digitize geographic data and represent the surface of the Earth by a graph. Multiple factors affecting cable path planning are considered through a summary cost which is a sum of the weighted costs of each of the factors. Then the least-cost path is derived by utilizing Dijkstra's algorithm [17].

In [18], Saito provided a node/link replacement strategy for a given planar physical cable network. In [19], Tran and Saito used seismic hazard information to develop an approach to find a set of geographical routes from candidate routes for a given cost constraint. Their objective was to maximize network robustness. Then, in [20], they considered how to add links and routes to an existing network so that the end-to-end disconnection probability is minimized for a given cost/budget limitation. This problem was solved using dynamic programming in [20]. In [21], a method for path selection from a set of candidate routes is provided. The method is based on Integer Linear Programming and minimizes expected cost for the cable owners as well as for the society when disaster strikes, where multiple cable breaks simultaneously in a given area are included. The work of [18]–[21] did not consider the shape of the cable (namely path planning) which is the focus of this paper.

More closely related publications are [9] and [22]–[26]. In [22], [24], and [25], a resilient path design for cables is proposed, but it is limited to cables that lie on a plane. In [26], a raster-based path analysis to find the least accumulative cost path using Dijkstra's algorithm for cable route selection, taking into account cost minimization and earthquake survivability, is given. A major limitation of the raster-based path approach is that a path is restricted to use either a lateral link or a diagonal link when moving from a cell to adjacent cells. In [9], we considered the fundamental problem of optimizing cable path planning between two points on the Earth's surface as a multiobjective optimization problem. We first converted the multiobjective optimization problem to a single objective optimization problem using the weighted sum method, and then transformed it to an Eikonal equation and solved it by FMM.

All the above mentioned publications, focused on design of homogenous cables. To the best of our knowledge, the only

work that has considered non-homogenous cables was in [27], [28], and [8]. In [27] and [28], Zhang *et al.* considered the problem of how to select submarine cables that require shielding in an existing cable network. Again, this work does not consider the shape of the cable. In [8], we considered the same problem of optimizing both the path planning and proper design levels, as in this paper. However, as discussed above, the algorithms proposed in [8] are raster-based and may not able to obtain solutions of acceptable quality in a reasonable running time for realistic large scale problems.

III. MODELS

Our aim is to design the path and select the design level of each point on the path of a cable γ between the starting node and the destination along the Earth's surface or buried in shallow ground. In this section, we describe the models we introduce for the landforms, laying cost, and the breakage risk, measured by the potential number of required repairs.

A. EARTH's SURFACE MODEL

As in [9], we use a *triangulated piecewise-linear two-dimensional manifold* $\mathbb{M}$ in $\mathbb{R}^3$ to approximate the Earth's surface. Each point on $\mathbb{M}$ is denoted by a three-dimensional coordinates (x, y, z), where $z = \xi(x, y)$ is the altitude of geographic location (x, y). For details of this representation, the reader can refer to [9].

B. LAYING COST MODEL

For a point $X = (x, y, z) \in \mathbb{M}, z = \xi(x, y)$, we use $u : \mathbb{M} \to \mathbb{U}$ to represent the design level at X. Without loss of generality, the design level variable u is assumed to take values of positive integers and $\mathbb{U} = \{1, 2, \ldots, L\}$ is assumed to be same for all the points on $\mathbb{M}$. The set of design levels for a cable is defined as $\mathcal{U} = \{u(\cdot) : \mathbb{M} \to \mathbb{U}\}$. We define a function $h(X, u)$ to represent the unit length laying cost of design level $u \in \mathbb{U}$ at X. The definition of $h(X, u)$ enables it to incorporate parameters associated with the location and the design level as dependent factors influencing laying cost. Examples for such parameters are the local site attributes (e.g. soil type, elevation, earth surface topography, etc.), which may affect cable survivability and ease of laying, as well as labor, licenses (e.g. right of way) and protection level.

As discussed, we aim to construct a cable (Lipschitz continuous [29]) γ to connect two nodes A and B in $\mathbb{M}$. The laying cost of the cable γ with design levels $u(\cdot) \in \mathcal{U}$ is represented by $\mathbb{H}(\gamma, u(\cdot))$. By the additive assumption of laying cost as in [9], $\mathbb{H}(\gamma, u(\cdot))$ can be represented as,

$$\mathbb{H}(\gamma, u(\cdot)) = \int_{\gamma} h\big(X, u(X)\big) ds. \tag{1}$$

Assigning appropriately high positive real numbers to the function $h(X, u)$ will enable avoidance of problematic areas [9].

C. CABLE REPAIR MODEL

In [9], the term *repair rate* is used to indicate the predicted number of repairs per unit length of the cable over a fixed time period into the future. In this paper, we extend the definition of repair rate function in [9] to include the design level variable u. The repair rate at location $X = (x, y, z) \in \mathbb{M}, z = \xi(x, y)$ is defined as $g(X, u),\ u \in \mathbb{U}$, where u is the design level at X. For the same location X on a cable, the repair rate caused by an earthquake is lower if higher design level is adopted, and vice versa. As discussed, a higher design level indicates higher laying cost and reduced number of repairs. In other words, $h(X, u_1) \leq h(X, u_2)$ and $g(X, u_1) \geq g(X, u_2)$ if $u_1 < u_2$ for any $X \in \mathbb{M}$.

As in [9], we accommodate the well-known high correlation between the repair rate and the ground motion intensity measure (e.g., Peak Ground Velocity). This is widely accepted in civil engineering [12]–[14]. Let $\mathbb{G}(\gamma, u(\cdot))$ denote the total number of repairs of a cable γ. Again, we assume that $\mathbb{G}(\gamma, u(\cdot))$ is additive. That is, $\mathbb{G}(\gamma, u(\cdot))$ can be rewritten as

$$\mathbb{G}(\gamma, u(\cdot)) = \int_{\gamma} g\,(X, u(X))\, ds, \tag{2}$$

where $g\,(X, u(X)) \in \mathbb{R}^1_+$ is the repair rate with a particular design level u at location X.

IV. PROBLEM FORMULATION AND SOLUTIONS

The laying cost model and the repair model above, lead to a formulation of a multiobjective optimization problem; minimization of both the laying cost and the total number of repairs as follows:

$$\min_{\gamma, u(\cdot)} \Phi(\gamma, u(\cdot)) = \big(\mathbb{H}(\gamma, u(\cdot)),\ \mathbb{G}(\gamma, u(\cdot))\big), \quad \text{(Problem 1)}$$
$$\text{s.t. } \gamma(A) = A,\ \gamma(B) = B,$$

where γ is the cable that connects Start Node A and Destination Point B and $u(\cdot) \in \mathcal{U}$ is the set of design levels for the cable γ.

For computing the two objectives of the cable γ, here we introduce the *natural parametrization* of a curve [30]: the curve γ is parameterized by a function of arc length denoted by s, and each point X on the cable γ can be represented by a function of s, i.e. $X = X(s)$. Using the natural parametrization of γ and redefine $u : \mathbb{R}_+ \cup \{0\} \to \mathbb{U}$, we can rewrite (1) and (2) as

$$\mathbb{H}(\gamma, u(\cdot)) = \int_0^{l(\gamma)} h\big(\gamma(s), u(s)\big) ds,$$
$$\mathbb{G}(\gamma, u(\cdot)) = \int_0^{l(\gamma)} g\big(\gamma(s), u(s)\big) ds, \tag{3}$$

where $h\big(\gamma(s), u(s)\big)$, $g\big(\gamma(s), u(s)\big)$ are the unit laying cost and the repair rate at location $\gamma(s)$ with a specified seismic design level $u(s)$, respectively, and $l(\gamma)$ represents the total length of the cable γ.

As discussed above, the two objectives, laying cost and the total number of repairs are conflicted, so that it is generally

impossible to simultaneously minimize both. A set of Pareto optimal solutions has to be sought. Note that if only one seismic design level is considered, i.e. $L = 1$, this problem is reduced to a multiobjective variational problem, studied in our previous work [9].

We convert Problem 1 into a single-objective optimization problem by weighting the two objectives as follows.

$$\min_{\gamma,u} \Phi'(\gamma, u(\cdot)) = \int_0^{l(\gamma)} f\left(\gamma(s), u(s)\right) ds, \qquad \text{(Problem 2)}$$
$$\text{s.t. } \gamma(0) = A, \gamma(l(\gamma)) = B,$$

where $f\left(\gamma(s), u(s)\right) = h\left(\gamma(s), u(s)\right) + c \cdot g\left(\gamma(s), u(s)\right)$ and $c \in \mathbb{R}_+^1 \cup \{0\}$.

The following theorem shows that a set of Pareto optimal solutions of Problem 1 can be obtained by solving Problem 2.

Theorem 1: If $(\gamma^*, u^*(\cdot))$ is an optimal solution for Problem 2, then it is Pareto optimal for the laying cost $\mathbb{H}$ and the total number of repairs $\mathbb{G}$.

Proof: See Appendix. ∎

For any point $S \in \mathbb{M}$, we define a cost function $\phi(S)$ that represents the minimal cumulative weighted cost to travel from End Point B of the cable to point S as

$$\phi(S) = \min_{\beta, u(\cdot)} \int_0^{l(\beta)} f\left(\beta(s), u(s)\right) ds, \tag{4}$$

where $\beta \in \text{Lip}([0, +\infty); \mathbb{M})$ is a Lipschitz continuous path parameterized by its length, $\|\beta'(s)\| = \|\frac{d\beta(s)}{ds}\| = 1$, $\beta(0) = B$, and $\beta(l(\beta)) = S$. By (4) and the definition of f, and applying the fundamental theorem of the calculus of variations, we next show that the optimal paths are the gradient descent contours of a specific Eikonal equation.

Theorem 2: $\phi(S)$ is the viscosity solution of the following Eikonal equation,

$$\|\nabla \phi(S)\| = \min_u f(S, u), \ \phi(B) = 0, \tag{5}$$

where ∇ is the gradient operator and $\|\cdot\|$ is the 2-norm.

Proof: See Appendix. ∎

For any point S, $\phi(S)$ is called the *level set function*; that is, $\{S \in \mathbb{M} : \phi(S) = a\}$ is a curve composed of all the points that can be reached from point B with minimal cost equal to a. The optimal path (s) is (are) along the gradient of $\phi(S)$; i.e., orthogonal to the level curves. Note that (5) is an extension to the Eikonal equation in [31]. From Problem 2 and (5), it can be observed that the joint optimization of the path γ and the design levels $u(\cdot)$ has been decomposed into two separate stages, of which the first stage is to calculate the minimum weighted cost value over all design levels for each point $S \in \mathbb{M}$, and the second stage is to solve the Eikonal equation.

In [9], we use FMM [10], [11], [31], [32], a computationally efficient and convergent algorithm, to solve the Eikonal equation without considering multiple design levels. Theorem 2 shows that FMM can be applied to solve Problem 2. The difference is that, for each point $S \in \mathbb{M}$, an additional step of calculating the minimum weighted cost value over all design levels; that is, $\min_{u \in \mathbb{U}} f(S, u)$, has to be executed before running FMM. This means for a fixed weight value c, once the minimum weighted cost value $f'(S) = \min_{u \in \mathbb{U}} f(S, u)$ for each $S \in \mathbb{M}$ is derived, we can input $f'(S)$ into the FMM, as in [9], and obtain the corresponding Pareto optimal solutions. By varying the weight value c in the calculation of the single combined objective function in Problem 2, a Pareto optimal set of Problem 1 is obtained. For the sake of completeness, we provide here the revised Algorithm 1 of [9] and to this end we present the full listing of the FMM-based method for Problem 2 as follows.

Algorithm 1 Algorithm for Optimization of Both the Path Planning and Design Levels in the Region of Interest $\mathbb{D}$

Require: Region $\mathbb{D}$ (modeled as $\mathbb{M}$), spatially distributed PGV data and laying cost data for each design level u on $\mathbb{D}$, mesh size Δ_x, Δ_y, Start Point A, End Point B, c, step size τ;

Ensure: Path γ and design level $u(\gamma)$ with minimum weighted cost;

1: Discretize $\mathbb{D}$ rectangularly with Δ_x in x and Δ_y in y, and denote the set of points on the grid by Γ;
2: Based on the PGV data on $\mathbb{D}$, calculate the repair rate $g(i, j, u)$ for each grid point $(i, j) \in \Gamma$ and design level u;
3: For each grid point $(i, j) \in \Gamma$, let $f'(i, j) = \min_u (h(i, j, u) + c \cdot g(i, j, u))$, where $h(i, j, u)$ is the laying cost at grid point (i, j) with design level u;
4: Create edges, faces and obtain a complete triangulation (i.e., $\mathbb{M}$) of $\mathbb{D}$ based on Γ;
5: Denote the approximate value of ϕ by $\bar{\phi}$ satisfying $\bar{\phi}(i, j) \simeq \phi(i\Delta_x + x_B, j\Delta_y + y_B)$. Let $\bar{\phi}(0, 0) = 0$ and set End Point B to *Near*. Define the neighbors of a grid element (i, j) to be the set $\Gamma_{(i,j)}$.
6: **while** *Near* list is not empty **do**
7: Find a point (i, j) with the minimum value $\bar{\phi}$ in *Near* list, and set it to be *Frozen*.
8: For each point $(i', j') \in \Gamma_{(i,j)}$, if (i', j') is not *Frozen*, for each face $\varsigma \in \Sigma$, $\Sigma = \{\varsigma, (i', j') \in \varsigma\}$, calculate $\bar{\phi}(i', j')$ and update its value with the minimum one using (10) or (11) in [9].
9: If (i', j') is *Far*, update its value by $\bar{\phi}(i', j')$ and add it in the *Near* list; otherwise update its value by minimum of $\bar{\phi}(i', j')$ and its current value.
10: **end while**
11: Let $\gamma_0 = A$ and $k = 0$.
12: **while** $||\gamma_k - B||^2 > \varepsilon$ **do**
13: Compute the gradient $G(\gamma_k)$ using finite-difference based on (6) in [9].
14: Compute $\gamma_{k+1} = \gamma_k - \tau G(\gamma_k)$, where γ_k is an approximation of $\gamma(t)$ at time $t = k\tau$.
15: Let $u(\gamma_{k+1})$ be the design level of the grid point nearest to γ_{k+1}.
16: **end while**
17: **return** γ and $u(\gamma)$.

Comparing with the multiobjective variational optimization problem without multiple design levels in [9], the only additional computational cost is caused by calculating $f'(S)$. Note that the computational complexity of FMM is $O(N \log(N))$, where N is the number of nodes in $\mathbb{M}$, enabling applicability to large scale problems. For details, the reader is referred to [9], [32], and [31].

V. APPLICATIONS AND NUMERICAL RESULTS

In this section, we apply the FMM-based method to two 3D realistic scenarios, Scenario B and Scenario C in [8]. Without loss of generality, we assume that there are two seismic design levels in these two scenarios; Levels 1 and 2 with low and high level protection, respectively. Considering the trade-off between the laying cost and the total number of repairs, the Pareto optimal solutions are obtained and the corresponding (approximate) Pareto front is generated. In addition, we compare the FMM-based method to the LS-based algorithm (Algorithm 1) and LS-IP algorithm in [8]. We run the codes in Matlab R2016b on a Lenovo ThinkCenter M900 Tower desktop (64 GB RAM, 3.4 GHz Intel(R) Core(TM) i7-6700 CPU).

A. THE FIRST SCENARIO

In this scenario, the objective region $\mathbb{D}$ is shown by Fig. 1; it is located in California from northwest (35.00° N, −118.00° E) to southeast (33.00° N, −116.00° E). The famous San Andreas fault line indicated by a red line in Fig. 1 cuts through the region $\mathbb{D}$. Our aim is to lay a cable connecting Start Point (33.55° N, −117.65° E) to End Point (35.00° N, −116.00° E) as shown in Fig. 1.

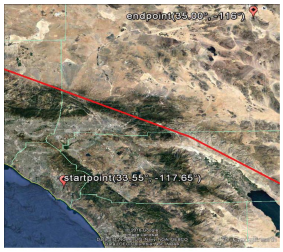

FIGURE 1. Region $\mathbb{D}$. Source: Google Earth.

The elevation data were downloaded from the General Bathymetric Chart of the Oceans (GEBCO) and the Peak Ground Acceleration (PGA) data were from USGS. The spatial resolution of the elevation data and the PGA data are 30 arc-second and 180 arc-second, respectively. For the specifications of the PGA data, the reader can refer to [8]. As in [8], the equation from Wald [33] is adopted to convert PGA to Peak Ground Velocity (PGV) for calculating repair rate of the cable as follows,

$$\log_{10}(v) = 1.0548 \cdot \log_{10}(\text{PGA}) - 1.5566, \tag{6}$$

where v (cm/s) represents the PGV value. Fig. 2 shows the obtained shaded PGV map of the region $\mathbb{D}$. [8, eqs. (6a) and (6b) and (7a) and (7b)] are used to calculate the repair rate and the laying cost measured by US dollars for the two design levels, respectively. Specifically, we assume that the laying costs per km for Level 1 and Level 2 are 1×10^4 US dollars and 2.22×10^4 US dollars, respectively. Note that the PGA statistics provided by USGS have been measured over a period of 50 years, so the estimated repair rate is over 50 years as well.

Observing Fig. 1 and Fig. 2, if we lay a cable from Start Point to End Point, it has to pass through a high risk area due to the existence of the San Andreas fault line. Since the spatial resolution of the PGA data is lower than that of the elevation data, and the computational complexity of the FMM-based method is lower than that of the LS-based algorithm, we first downsample the elevation data to the level of the resolution of the PGA data (i.e., 180 arc-second) in order to compare the FMM-based method with the LS-based algorithm. We therefore use two sets of data: the original PGA data and the downsampled elevation data, which we call the low-precision data. To show the benefit of deriving a better approximation to the Pareto front using high resolution data and to take advantage of the computational efficiency of the FMM-based method, we then generate the so-called high-precision data by interpolating the PGA data (i.e., complementing missing data by interpolation) to make it have the same spatial resolution as the original elevation data (i.e., 30 arc-second). Then, we apply the FMM-based method to both the low-precision data and the high-precision data. Recall that, the LS-based algorithm is applied to the low-precision data only since it can not be used to obtain the Pareto front in a reasonable time for the high-precision data. Thereafter, we compare the LS-based algorithm using the low-precision data with the FMM-based method.

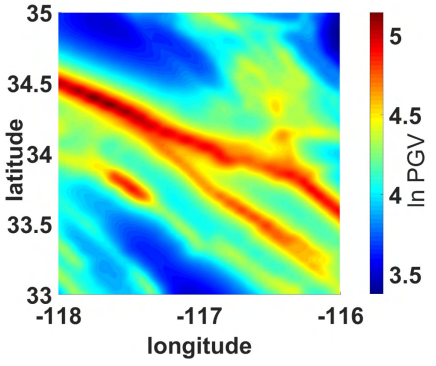

FIGURE 2. Logarithmic PGV map of the objective region $\mathbb{D}$.

Several Pareto optimal paths using high-precision data are shown in Fig. 3 and the corresponding laying cost $\mathbb{H}(\gamma^*, u^*(\cdot))$ and the total number of repairs $\mathbb{G}(\gamma^*, u^*(\cdot))$ are shown in Table 1. In Fig. 3, the 3D topographic landform shown is on the left and the corresponding 2D logarithmic PGV from top view is on the right, where magenta lines indicate the cable or cable segments adopting Level 1 and

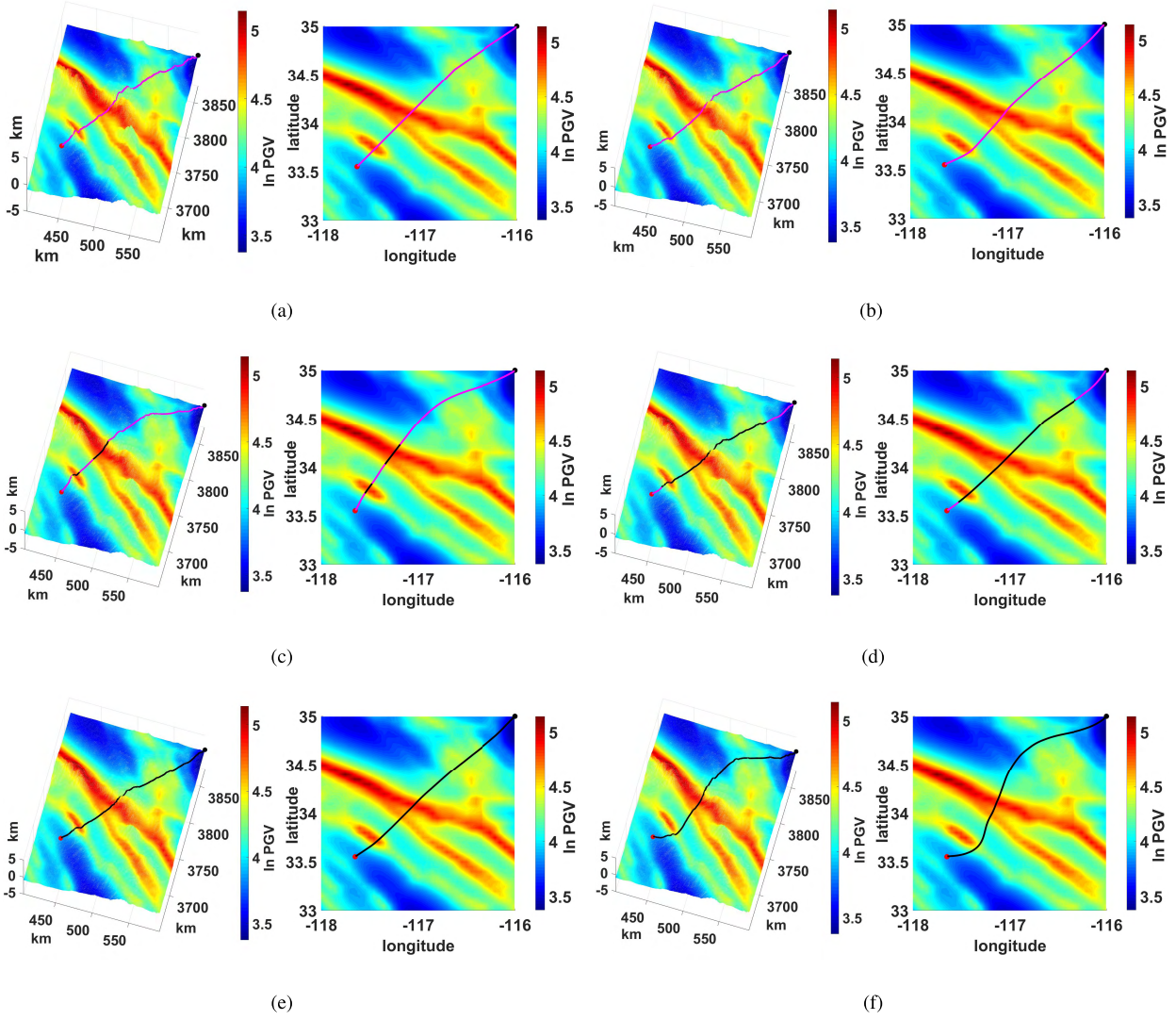

FIGURE 3. Selected Pareto optimal paths (obtained by FMM-based method) of the first scenario. The magenta lines represent the path or path segments adopting Level 1 and the black lines represent the path or path segments adopting Level 2.

the black lines indicate the cable or cable segments adopting Level 2.

From Table 1, we can see the trade-off between the laying cost and the total number of repairs. In order to generate the (approximate) Pareto front, we vary the weight value c from 0 to 1000. As the weight value c increases, the laying cost increases and the total number of repairs decreases. In other words, the higher the laying cost, the lower the total number of repairs. It is observed that, to reduce risk (lower number of repairs), we can either add segments with high level protection (see the black lines in Fig. 3(c)) or increase the length of the cable to avoid the high risk areas shown by Fig. 3(b). We can also observe that the laying cost increases and the total number of repairs decreases when some parts of the cable have high level protection. From Fig. 3(a) and Fig. 3(b), the cable is designed to keep away from the high PGV areas to reduce the total number of repairs. However, it appears from Table 1 that avoiding the high PGV areas is not very effective in decreasing the total number of repairs of the cable. In this scenario, the San Andreas fault line cuts through the objective region $\mathbb{D}$. This implies that the designed path has to pass through the high PGV areas and a higher design level should be adopted for the cable deployed

TABLE 1. Laying cost (in units of 10^4 US dollars) and total number of repairs of selected Pareto optimal paths of the first scenario.

	c	$\mathbb{H}(\gamma^*, u^*(\cdot))$	$\mathbb{G}(\gamma^*, u^*(\cdot))$
a	0	220.7205	42.5164
b	3.8	222.3874	41.6799
c	6.2	276.6942	29.6408
d	10.5	421.0422	13.0290
e	24	491.5129	8.5157
f	500	534.2173	8.0231

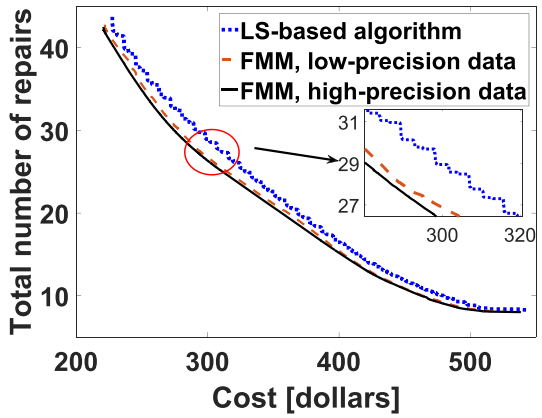

FIGURE 4. Pareto front for the two objectives: (1) laying cost (in units of 10^4 US dollars), and (2) total number of repairs of the first scenario.

TABLE 2. Laying cost (in units of 10^4 US dollars) and the total number of repairs of selected paths of the FMM-based method and the LS-based algorithm.

	$\mathbb{H}(\gamma^*, u^*(\cdot))$	$\mathbb{G}(\gamma^*, u^*(\cdot))$
LS-based algorithm	304.1759	28.4903
FMM-based method (high-precision data)	284.0619	28.5005

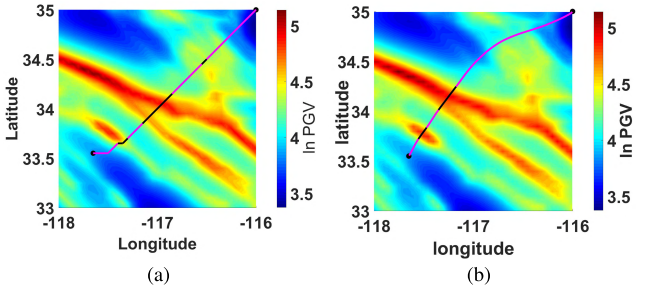

FIGURE 5. Two paths obtained by the FMM-based method using the high-precision data and the LS-based algorithm. (a) LS-based algorithm. (b) FMM-based method.

in such high risk areas. Adopting a higher design level for some parts of the cable is noticeable, and these higher level protected segments become longer around the high PGV areas as shown by Fig. 3(c) and Fig. 3(d). The reduction of the total number of repairs is significant but with an increased laying cost by the deployment of a higher design level for the cable.

The (approximate) Pareto fronts obtained by the FMM-based method using the low-precision data and the high-precision data, consisting of 451 points and 841 points, respectively, are shown by the brown dash line and the black solid line in Fig. 4. The FMM-based method that uses data with higher precision generates more accurate path planning and a better approximation for the Pareto front. The blue dotted line in Fig. 4 shows the Pareto front (consisting of 1381 points) obtained by the LS-based algorithm using the

FIGURE 6. Region $\mathbb{D}'$. Source: Google Earth.

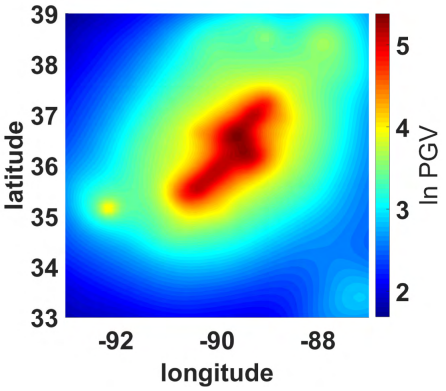

FIGURE 7. Logarithmic PGV map of the objective region $\mathbb{D}'$.

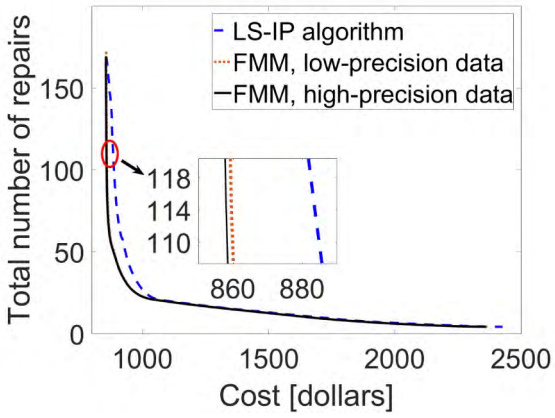

FIGURE 8. Pareto front for the two objectives: (1) laying cost (in units of 10^4 US dollars), and (2) total number of repairs of the second scenario.

low-precision data. It is seen that, for the same total number of repairs, the laying costs obtained by the FMM-based method using both the low-precision data and the high-precision data are smaller than that obtained by the LS-based algorithm. From Fig. 4, if we set the total number of repairs the same and larger than 15, commonly the laying cost obtained by the FMM-based method using high-precision data will be reduced approximately by 4% comparing with the LS-based algorithm. This reduction increases to about 6.5% if the total

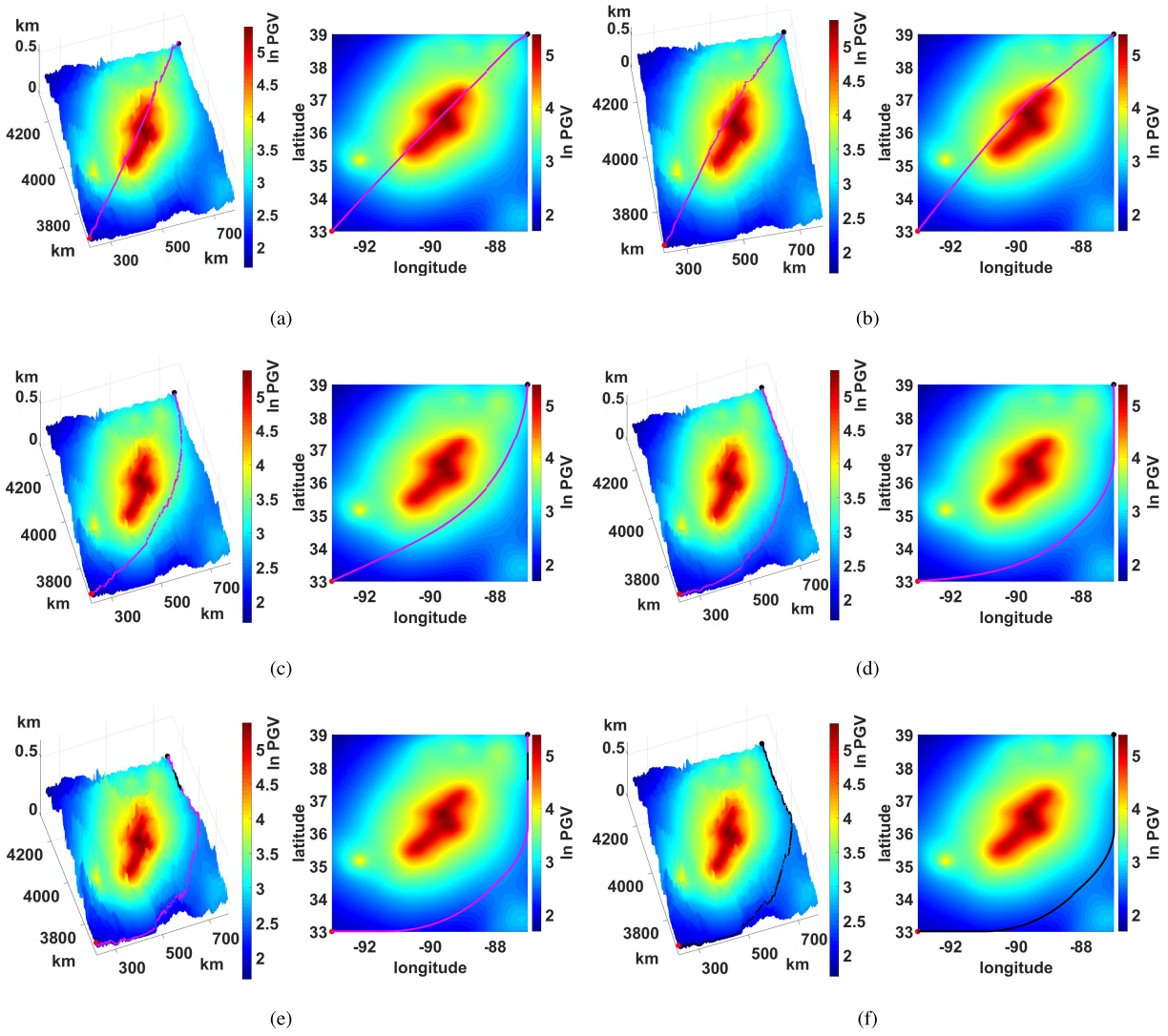

FIGURE 9. Selected Pareto optimal paths (obtained by FMM-based method) of the second scenario. The magenta lines represent the path or path segments adopting Level 1 and the black lines represent the path or path segments adopting Level 2.

number of repairs is set in the range of 25 to 30. As an example, Fig. 5 shows two paths, one obtained by the FMM-based method using the high-precision data and the other by the LS-based algorithm, respectively, with very similar total number of repairs as shown in Table 2. The laying cost reduction is up to 6.61%. This difference is significant considering the billions of dollars spent around the world on telecommunications cabling. Although the total number of repairs of the two cables are very close, their corresponding paths are quite different.

In terms of the computational cost, it takes 251s and 5,192s for the FMM-based method to obtain the (approximate) Pareto fronts using the low-precision data and the high-precision data, respectively. The running time of the LS-based algorithm is 2,409s for the low-precision data. As a result, bearing in mind the higher quality solution from the FMM-based method, it is difficult to make a case for the LS-based algorithm.

B. THE SECOND SCENARIO

In this scenario, we consider a large scale realistic landform in central USA. The objective region $\mathbb{D}'$, shown by Fig. 6, is from the southwest corner (33.00° N,−93.00° E) to northeast corner (39.00° N, −87.00° E). The New Madrid fault line, represented by the black lines in Fig. 6, is located in the central of $\mathbb{D}'$. The logarithmic PGV map of region $\mathbb{D}'$ is shown by Fig. 7. Our aim is to design the path for a cable from the southwest corner (33.00° N,−93.00° E) to the northeast corner (39.00° N, −87.00° E).

Again, we downsample the elevation data or interpolating the PGA data to generate the low-precision data (i.e., 120 arc-second spatial resolution) and the high-precision data (i.e., 30 arc-second spatial resolution). The (approximate) Pareto fronts (consisting of 754 points and 823 points), obtained by the FMM-based method using the low-precision data and the high precision data through varying the weight value c from 0 to 1200, are shown by the brown dotted line and the black

solid line in Fig. 8, respectively. From Fig. 8, the (approximate) Pareto fronts obtained using the low-precision data and the high-precision data are very close. Several selected optimal paths obtained by the FMM-based method using the high-precision data are shown in Fig. 9 and the corresponding laying cost and the total number of repairs are shown in Table 3. Unlike in the first scenario, to reduce the total number of repairs of the cable in this scenario, avoiding the high PGV areas is much more effective than adopting a higher design level since the designed path can totally avoid the high PGV areas through deploying a longer cable as shown by Fig. 9(c) and Fig. 9(d).

TABLE 3. Laying cost (in units of 10^4 US dollars) and total number of repairs of selected Pareto optimal paths of the second scenario.

	c	$\mathbb{H}(\gamma^*, u^*(\cdot))$	$\mathbb{G}(\gamma^*, u^*(\cdot))$
a	0	856.1859	169.0890
b	0.08	858.5708	105.4468
c	3	915.8192	36.8502
d	20	1013.4469	21.8293
e	50	1159.4206	18.3306
f	800	2347.7978	4.1533

The raster-based LS-based algorithm is not applicable for such a large scale landform even when the low-precision data are used. Instead, by setting $\varepsilon = 0.8$, we run the LS-IP algorithm of [8] using the low-precision data, obtaining the Pareto front (consists of 336 points) shown by the blue dash line in Fig. 8. Note that the number of nodes of the generated graph is too large to obtain the Pareto front for LS-IP if the high-precision data are used. From Fig. 8, it is observed that the FMM-based method performs at least as well as the LS-IP algorithm. If we set the total number of repairs in the range of 25 to 100, typically a more than 3.5% laying cost reduction is obtained by applying the FMM-based method. Considering that over 100,000 km of optical fiber cables are laid every year at a cost of billions of dollars, this improvement is still significant.

Regarding computational cost, the running time for the FMM-based method using the low-precision data, the high-precision data and LS-IP, are 1,308s, 62,526s and 15,334s, respectively. It is seen, again, that the FMM-based method has much better performance than LS-IP on computational cost if we use the same data.

Based on the two above mentioned scenarios, we conclude that the FMM-based method not only performs better on finding the approximate Pareto front, but also runs much faster than the LS-based algorithm and the LS-IP algorithm. For Problem 1 with a very large scale landform, the FMM-based method can be adopted because of its efficiency and solution quality.

VI. CONCLUSION

We have considered the path optimization and non-homogenous construction problem for a cable connecting two points on Earth's surface with high risk areas when multiple design levels are available. Taking account of laying cost and total number of repairs of the cable as the two objectives, we have formulated the problem as a variant of the multiobjective variational optimization problem. The Earth's surface has been modeled by a triangulated piecewise-linear two-dimensional manifold in $\mathbb{R}^3$ and the repair rate has been calculated by ground motion intensity measures of earthquake events. We have solved the multiobjective variational optimization problem leveraging FMM, and have obtained (approximate) Pareto fronts for the two objectives for a range of numerical experiments. Comparing with the existing raster-based algorithms, namely, the LS-based algorithm and the LS-IP algorithm in [8], the FMM-based method has better performance both on the approximation of Pareto fronts and the computational cost.

APPENDIX

Proof of Theorem 1: Suppose $(\gamma^*, u^*(\cdot))$ is not Pareto optimal for the laying cost $\mathbb{H}$ and the total number of repairs $\mathbb{G}$. This means that there exists a feasible solution $(\gamma, u(\cdot))$ such that $\mathbb{H}(\gamma, u(\cdot)) < \mathbb{H}(\gamma^*, u^*(\cdot))$ and $\mathbb{G}(\gamma, u(\cdot)) \leq \mathbb{G}(\gamma^*, u^*(\cdot))$, or $\mathbb{H}(\gamma, u(\cdot)) \leq \mathbb{H}(\gamma^*, u^*(\cdot))$ and $\mathbb{G}(\gamma, u(\cdot)) < \mathbb{G}(\gamma^*, u^*(\cdot))$. Since the weight $c > 0$, we have $\mathbb{H}(\gamma, u(\cdot)) + c \cdot \mathbb{G}(\gamma, u(\cdot)) < \mathbb{H}(\gamma^*, u^*(\cdot)) + c \cdot \mathbb{G}(\gamma^*, u^*(\cdot))$. This contradicts the assumption that $(\gamma^*, u^*(\cdot))$ is a solution of Problem 2 and, thus, $(\gamma^*, u^*(\cdot))$ must be Pareto optimal for Problem 1. □

Proof of Theorem 2: Note that we assume the cable is laid on a two-dimensional manifold $\mathbb{M}$ in three-dimensional Euclidean space $\mathbb{R}^3$. We have

$$\int_0^{l(\beta)} f(\beta(s), u(s))ds = \int_0^1 f(x(t), y(t), u(t))(x'^2(t) + y'^2(t))^{\frac{1}{2}} dt, \tag{7}$$

where $ds = (x'^2(t) + y'^2(t))^{\frac{1}{2}} dt$, ds is an arbitrarily small arc length, and t is an arbitrary parameterization of the curve β. By fundamental calculus of variations, we obtain the following three Euler-Lagrange equations.

$$\begin{aligned} &\frac{\partial f}{\partial x}(x'^2 + y'^2)^{\frac{1}{2}} - \frac{d}{ds}\left(f \cdot \frac{x'}{(x'^2 + y'^2)^{\frac{1}{2}}}\right) = 0, \\ &= \frac{\partial f}{\partial y}(x'^2 + y'^2)^{\frac{1}{2}} - \frac{d}{ds}\left(f \cdot \frac{y'}{(x'^2 + y'^2)^{\frac{1}{2}}}\right) = 0, \\ &= \frac{\partial f}{\partial u} = 0. \end{aligned} \tag{8}$$

The curvature κ of the curve β is given by [34]

$$\kappa = \frac{x'y'' - x''y'}{(x'^2 + y'^2)^{\frac{3}{2}}} \tag{9}$$

with $x'' = \frac{d^2x}{dt^2}$, $y'' = \frac{d^2y}{dt^2}$. Therefore,

$$\frac{d}{dt}\left(\frac{x'}{(x'^2+y'^2)^{\frac{1}{2}}}\right) = -\kappa y',$$
$$\frac{d}{dt}\left(\frac{y'}{(x'^2+y'^2)^{\frac{1}{2}}}\right) = \kappa x'. \quad (10)$$

Substituting the two equations in (10) into the first two equations of (8), respectively, yields,

$$\frac{\partial f}{\partial x}(x'^2+y'^2)^{\frac{1}{2}} - \frac{df}{dt}\frac{x'}{(x'^2+y'^2)^{\frac{1}{2}}} + f\kappa y' = 0,$$
$$\frac{\partial f}{\partial y}(x'^2+y'^2)^{\frac{1}{2}} - \frac{df}{dt}\frac{y'}{(x'^2+y'^2)^{\frac{1}{2}}} - f\kappa x' = 0. \quad (11)$$

Multiplying the first equation of (11) by y', and then subtracting by the multiplication of second equation of (11) with x', yields

$$\left(\frac{\partial f}{\partial x}(x'^2+y'^2)^{\frac{1}{2}} + f\kappa y'\right)y' = \left(\frac{\partial f}{\partial y}(x'^2+y'^2)^{\frac{1}{2}} - f\kappa x'\right)x'. \quad (12)$$

Combining with the third equation of (8), we obtain the following Euler-Lagrange geometric equation,

$$\kappa f|_{u=u_{\min}} = < \nabla f|_{u=u_{\min}}, \mathbf{n} >, \quad (13)$$

where $\mathbf{n} = (-\frac{y'}{\sqrt{x'^2+y'^2}}, \frac{x'}{\sqrt{x'^2+y'^2}})$ is the unit normal of β, ∇ is the gradient operator, and $f|_{u=u_{\min}} = \min_{u\in\mathbb{U}} f(S,u)$ is the minimum value function of f with respect to $u \in \mathbb{U}$.

Based on the Euler-Lagrange geometric equation (13), our subsequent proof follows [35, Lemma 1] by replacing the function g with $f|_{u=u_{\min}}$. □

REFERENCES

[1] TeleGeography. (2016). *Submarine Cable Map*. [Online]. Available: https://www.telegeography.com/telecom-maps/submarine-cable-map/index.html

[2] K. Nielsen, "Submarine telecoms industry report," Submarine Telecoms Forum, Richmond, VA, USA, Tech. Rep. Issue 4, 2015.

[3] W. Qiu. (Mar. 2011). *Submarine Cables Cut after Taiwan Earthquake in Dec 2006*. [Online]. Available: http://www.submarinenetworks.com

[4] T. P. Dübendorfer, "Impact analysis, early detection and mitigation of large-scale Internet attacks," Ph.D. dissertation, Dipl. Informatik-Ing., ETH Zürich, Zürich, Switzerland, 2005.

[5] T. Davenport, "Submarine communications cables and law of the sea: Problems in law and practice," *Ocean Develop. Int. Law*, vol. 43, no. 3, pp. 201–242, 2012.

[6] D. R. Burnett, R. Beckman, and T. M. Davenport, *Submarine Cables: The Handbook of Law and Policy*. Leiden, The Netherlands: Martinus Nijhoff, 2013.

[7] A. Al-Lawati, "Fiber optic submarine cables cuts cost modeling and cable protection aspects," *Opt. Fiber Technol.*, vol. 22, pp. 68–75, Mar. 2015.

[8] Z. Wang, Q. Wang, M. Zukerman, and B. Moran, "A seismic resistant design algorithm for laying and shielding of optical fiber cables," *J. Lightw. Technol.*, vol. 35, no. 14, pp. 3060–3074, Jul. 15, 2017.

[9] Z. Wang *et al.*, "Multiobjective path optimization for critical infrastructure links with consideration to seismic resilience," *Comput.-Aided Civil Infrastruct. Eng.*, vol. 32, no. 10, pp. 836–855, Oct. 2017.

[10] J. A. Sethian, "A fast marching level set method for monotonically advancing fronts," *Proc. Nat. Acad. Sci. USA*, vol. 93, no. 4, pp. 1591–1595, 1996.

[11] R. Kimmel and J. Sethian, "Fast marching methods on triangulated domains," *Proc. Nat. Acad. Sci. USA*, vol. 37, no. 1, pp. 5253–5261, 1998.

[12] Y. Wang and T. D. O'Rourke, "Seismic performance evaluation of water supply systems," Multidiscipl. Center Earthquake Eng. Res., Buffalo, NY, USA, Tech. Rep. MCEER-08-0015, 2008.

[13] M. Fragiadakis and S. E. Christodoulou, "Seismic reliability assessment of urban water networks," *Earthq. Eng. Struct. Dyn.*, vol. 43, no. 3, pp. 357–374, 2014.

[14] S.-S. Jeon and T. D. O'Rourke, "Northridge earthquake effects on pipelines and residential buildings," *Bull. Seismol. Soc. Amer.*, vol. 95, no. 1, pp. 294–318, 2005.

[15] E. Tahchi, private communication, Oct. 2016.

[16] J. Luettinger and T. Clark, "Geographic information system-based pipeline route selection process," *J. Water Resour. Planning Manage.*, vol. 131, no. 3, pp. 193–200, 2005.

[17] S. R. Wasi and J. D. Bender, "Spatially enabled pipeline route optimization model," in *Proc. Int. Pipeline Conf.*, 2004, pp. 699–707.

[18] H. Saito, "Analysis of geometric disaster evaluation model for physical networks," *IEEE/ACM Trans. Netw.*, vol. 23, no. 6, pp. 1777–1789, Dec. 2015.

[19] P. N. Tran and H. Saito, "Geographical route design of physical networks using earthquake risk information," *IEEE Commun. Mag.*, vol. 54, no. 7, pp. 131–137, Jul. 2016.

[20] P. N. Tran and H. Saito, "Enhancing physical network robustness against earthquake disasters with additional links," *J. Lightw. Technol.*, vol. 34, no. 22, pp. 5226–5238, Nov. 15, 2016.

[21] D. L. Msongaleli, F. Dikbiyik, M. Zukerman, and B. Mukherjee, "Disaster-aware submarine fiber-optic cable deployment for mesh networks," *J. Lightw. Technol.*, vol. 34, no. 18, pp. 4293–4303, Sep. 15, 2016.

[22] W. Wu, B. Moran, J. H. Manton, and M. Zukerman, "Topology design of undersea cables considering survivability under major disasters," in *Proc. Adv. Inf. Netw. Appl. Workshops (WAINA)*, Bradford, U.K., May 2009, pp. 1154–1159.

[23] C. Cao, M. Zukerman, W. Wu, J. H. Manton, and B. Moran, "Survivable topology design of submarine networks," *J. Lightw. Technol.*, vol. 31, no. 5, pp. 715–730, Mar. 1, 2013.

[24] C. Cao, "Cost effective and survivable cabling design under major disasters," Ph.D. dissertation, Dept. Electron. Eng., City Univ. Hong Kong, Hong Kong, 2015.

[25] C. Cao, Z. Wang, M. Zukerman, J. Manton, A. Bensoussan, and Y. Wang, "Optimal cable laying across an earthquake fault line considering elliptical failures," *IEEE Trans. Rel.*, vol. 65, no. 3, pp. 1536–1550, Sep. 2016.

[26] M. Zhao, T. W. S. Chow, P. Tang, Z. Wang, J. Guo, and M. Zukerman, "Route selection for cabling considering cost minimization and earthquake survivability via a semi-supervised probabilistic model," *IEEE Trans. Ind. Informat.*, vol. 13, no. 2, pp. 502–511, Apr. 2017.

[27] J. Zhang, E. Modiano, and D. Hay, "Enhancing network robustness via shielding," in *Proc. 11th Int. Conf. Des. Reliable Commun. Netw. (DRCN)*, Mar. 2015, pp. 17–24.

[28] J. Zhang, E. Modiano, and D. Hay, "Enhancing network robustness via shielding," *IEEE/ACM Trans. Netw.*, vol. 25, no. 4, pp. 2209–2222, Aug. 2017.

[29] K. Eriksson, D. Estep, and C. Johnson, *Applied Mathematics: Body and Soul: Derivatives and Geometry in IR3*, vol. 1. New York, NY, USA: Springer, 2004.

[30] D. Burago, Y. Burago, and S. Ivanov, *A Course in Metric Geometry*, vol. 33. Providence, RI, USA: AMS, 2001.

[31] J. Sethian, "Fast marching methods," *SIAM Rev.*, vol. 41, no. 2, pp. 8431–8435, 1998.

[32] J. Sethian, *Level Set Methods and Fast Marching Methods: Evolving Interfaces in Computational Geometry Fluid Mechanics* (Computer Vision, and Materials Science), 2nd ed. New York, NY, USA: Cambridge Univ. Press, 1999.

[33] D. J. Wald, V. Quitoriano, T. H. Heaton, and H. Kanamori, "Relationships between peak ground acceleration, peak ground velocity, and modified Mercalli intensity in California," *Earthq. Spectra*, vol. 15, no. 3, pp. 557–564, Aug. 1999.

[34] M. P. Do Carmo and M. P. Do Carmo, *Differential Geometry of Curves and Surfaces*, vol. 2. Englewood Cliffs, NJ, USA: Prentice-Hall, 1976.

[35] R. Kimmel and J. Sethian, "Optimal algorithm for shape from shading and path planning," *J. Math. Imag. Vis.*, vol. 14, no. 3, pp. 237–244, 2001.

ZENGFU WANG received the B.Sc. degree in applied mathematics, the M.Sc. degree in control theory and control engineering, and the Ph.D. degree in control science and engineering from Northwestern Polytechnical University, Xi'an, in 2005, 2008, and 2013, respectively. He was a Lecturer with Northwestern Polytechnical University from 2014 to 2017. He is currently an Associate Professor with Northwestern Polytechnical University. His research interests include path planning, discrete optimization, and information fusion.

QING WANG received the B.Eng. degree in control science and engineering from Zhejiang University, Hangzhou, in 2014. He is currently pursuing the Ph.D. degree in electrical engineering with the City University of Hong Kong, Hong Kong.

BILL MORAN (M'95) received the B.Sc. degree (Hons.) in mathematics from the University of Birmingham in 1965 and the Ph.D. degree in pure mathematics from the University of Sheffield, U.K., in 1968. He was a Professor of mathematics from 1976 to1991, the Head of the Department of Pure Mathematics from 1977 to 1979 and from 1984 to 1986, the Dean of mathematical and computer sciences, University of Adelaide, in 1981, 1982, and 1989, and the Head of the mathematics discipline, Flinders University of South Australia from 1991 to 1995. He was a Chief Investigator from 1992 to1995, and the Head of the Medical Signal Processing Program with the Cooperative Research Centre for Sensor Signal and Information Processing from 1995 to 1999. He has been a Professor with the Department of Electrical and Electronic Engineering, The University of Melbourne, since 2001. He was the Research Director of the Defense Science Institute, The University of Melbourne, from 2011 to 2014. He was a Professor and the Director of the Signal Processing and Sensor Control Group, School of Engineering, RMIT University, Australia from 2014 to 2017. He currently serves as a Professor with the Department of Electrical and Electronic Engineering, The University of Melbourne, Australia. He has been a Principal Investigator on numerous research grants and contracts, in areas spanning pure mathematics to radar development, from both Australian and US Research Funding Agencies, including DARPA, AFOSR, AFRL, the Australian Research Council, the Australian Department of Education, Science and Training, and DSTO. His main areas of research interest are in signal processing both theoretically and in applications to radar, waveform design and radar theory, sensor networks, and sensor management. He also works in various areas of mathematics, including harmonic analysis, representation theory, and number theory. He is a member of the Australian Research Council College of Experts. He was elected to the Fellowship of the Australian Academy of Science in 1984.

MOSHE ZUKERMAN (M'87–SM'91–F'07) received the B.Sc. degree in industrial engineering and management and the M.Sc. degree in operations research from the Technion—Israel Institute of Technology, Haifa, Israel, and the Ph.D. degree in engineering from University of California, Los Angeles, in 1985. He was an independent Consultant with the IRI Corporation and a Post-Doctoral Fellow with the University of California, Los Angeles, from 1985 to 1986. From 1986 to 1997, he was with Telstra Research Laboratories, first as a Research Engineer and from 1988 to 1997, as a Project Leader. He also taught and supervised graduate students at Monash University from 1990 to 2001. From 1997 to 2008, he was with The University of Melbourne, Melbourne, Australia. In 2008, he joined the City University of Hong Kong as a Chair Professor of information engineering, and a Team Leader. He has over 300 publications in scientific journals and conference proceedings. He has served on various editorial boards, such as *Computer Networks*, the IEEE *Communications Magazine*, the IEEE JOURNAL OF SELECTED ARES IN COMMUNICATIONS, the IEEE/ACM TRANSACTIONS ON NETWORKING, and the *International Journal of Communication Systems*.